Forecasting the Term Structure of Interest Rates with Potentially Misspecified Models*

Yunjong Eo† University of Sydney

Kyu Ho Kang‡ Korea University

August 2016

Abstract

This paper assesses the predictive gains of the pooling method in yield curve prediction. We consider three individual yield curve prediction models: the dynamic Nelson-Siegel model (DNS), the arbitrage-free Nelson-Siegel model, and the random walk (RW) model as a benchmark. Despite the popularity of these three frameworks, none of them dominates the others across all maturities and forecast horizons. This fact indicates that the models are potentially misspecified. We investigate whether combining the possibly misspecified models in a linear form and in a Markov-switching mixture helps improve predictive accuracy. To do this, we evaluate the out-of-sample forecasts of the pooled models compared to the individual models. In terms of density prediction, the pooled model of the DNS and RW models consistently outperforms the individual models regardless of maturities and forecast horizons. Our findings provide strong evidence that the pooling method can be a better option than selecting one of the alternative models. We also find that the RW model has been important in improving the forecasting accuracy since 2009.

JEL classification: G12, C11, F37
Keywords: Model combination, Markov-switching mixture, Dynamic Nelson-Siegel, Affine term structure model

*We thank Gianni Amisano, Graham Elliott, Helmut Lütkepohl, James Morley, Tara Sinclair, and seminar and conference participants at Texas A&M University, the Federal Reserve Bank of Dallas, the Reserve Bank of New Zealand, University of California, Riverside, Hitotsubashi University, the Bank of Korea, the Society for Nonlinear Dynamics and Econometrics Conference, Recent Developments in Financial Econometrics and Applications, EFaB@Bayes 250 Workshop, and Econometric Society Australasian Meeting for useful feedback. All remaining errors are our own.

†School of Economics, University of Sydney, NSW 2006, Australia; Tel: +61 2 9351 3075; Email: yunjong.eo@sydney.edu.au

‡Department of Economics, Korea University, Seoul, South Korea, 136-701; Tel: +82 2 3290 5132; Email: kyuho@korea.ac.kr

1 Introduction

Forecasting the yield curve is extremely important for bond portfolio risk management, monetary policy, and business cycle analysis. In the previous literature, three classes of yield curve prediction models have been widely used. One is the arbitrage-free affine term structure model, which is a theoretical bond pricing approach.[1] This approach provides many economically interpretable outcomes such as term premium and term structure of real interest rates. Despite its flexibility and microfoundation, this class of models is known to be difficult to estimate because of its nonlinearity and irregular likelihood surface.

Another approach is a purely statistical, dynamic version of the Nelson-Siegel (DNS) model.[2] Since this modeling approach is parsimonious but flexible for fitting the yield curve, its forecasting performance is better than the theoretical approach overall. The final approach is the random-walk model (RW), which is often used as a benchmark in forecasting ability.

Beating the RW is a challenging task, although the DNS or the arbitrage-free term structure model can be better for some particular maturities and forecast horizons. None of the three alternative models uniformly outperforms the other models for all maturities and forecast horizons. For example, Diebold and Li (2006) find that the three-factor DNS outperforms the RW at the one-month-ahead horizon for short maturities but, for long-term bond yields, the RW dominates the DNS. Zantedeschi et al. (2011) confirm that the RW forecasts better in the short run whereas at three- and six-step-ahead forecast horizons, the predictions from their DNS with time-varying factor loadings are much improved. Moench (2008) finds that the arbitrage-free affine term structure model forecasts better than the RW at the six-month maturity only. Using an affine term structure model, Carrieroa and Giacomini (2011) produce one-step-ahead forecasts and find positive prediction gains against the RW at intermediate and long maturities, not at short maturities.

[1] For example, Moench (2008), Christensen, Diebold, and Rudebusch (2011), Chib and Kang (2013), Almeida and Vicenteb (2008), and Carrieroa and Giacomini (2011).

[2] For example, Diebold and Li (2006), De Pooter (2007), and Zantedeschi, Damien, and Polson (2011).

These mixed results for out-of-sample prediction comparisons strongly indicate that all the prediction models are potentially somewhat misspecified and the model uncertainty is enormous. The goal of this paper is to investigate whether it is possible to improve out-of-sample prediction performance when all alternative models are potentially misspecified. In a Bayesian context a standard way to consider the model uncertainty is by using the Bayesian model-averaging method based on the marginal likelihood computation. As Del Negro, Hasegawa, and Schorfheide (2016) point out, however, Bayesian model averaging typically gives a weight of nearly one on one of the individual models, excluding the other models.

As an alternative way to consider the model misspecifications we take the pooling method recently suggested by Geweke and Amisano (2011), Geweke and Amisano (2012) and Waggoner and Zha (2012). The central idea of this approach is to construct the one-step-ahead predictive density as a linear combination of the predictive densities obtained from each of the alternative prediction models. In this paper the three individual yield curve prediction models and pooled models of two or three of the individual models are compared in terms of out-of-sample predictive accuracy. When considering the pooling approach, the weights are equally given to be estimated as constant parameters, or they follow the first-order Markov-switching process. Using these pooled models, we forecast the monthly yields with eight different maturities over the forecast horizons of one through twelve months and conduct a model comparison analysis using the root mean squared error and the posterior predictive criterion.

According to our empirical experiments based on 108 out-of-sample periods, the pooled model of the DNS and RW with equal model weights dominates all individual models across all maturities and forecast horizons in terms of bond yield density forecasting. Moreover, the predictive gains using the pooling method are remarkable. In contrast, for the point forecasting, we do not find strong evidence that the pooling method can help improve the predictive accuracy. Our findings strongly indicate that, for density prediction, the pooling method is worth trying, and that the pooled models should be examined before one of them is selected.

The remainder of the paper is organized as follows. Section 2 briefly describes our

pooling methods, and Section 3 specifies all competing models including the three individual prediction models and the pooled models. In Section 4, we present our Bayesian Markov chain Monte Carlo (MCMC) algorithm for estimation. Sections 5 and 6 provide the empirical results and discuss their implications. Finally, Section 7 concludes the paper.

2 Pooling Method

In this section we illustrate the pooling method using an example of two prediction models, $\mathcal{M}_1$ and $\mathcal{M}_2$. Let Θ_1 and Θ_2 be the set of parameters in $\mathcal{M}_1$ and $\mathcal{M}_2$, respectively. The set of maturities is $\{\tau_i\}_{i=1}^N$, the τ-period bond yield at time t is denoted by $y_t(\tau)$, and the vector of yields with N different maturities at time t is

$$\mathbf{y}_t = (y_t(\tau_1), y_t(\tau_2), .., y_t(\tau_N))'.$$

We let $Y_t = \{y_i\}_{i=1}^t$ denote the observed yield curve data up to time t. Then, Geweke and Amisano (2011) study predictive densities of the form

$$w_1 \times p(\mathbf{y}_t|Y_{t-1}, \Theta_1, \mathcal{M}_1) + (1 - w_1) \times p(\mathbf{y}_t|Y_{t-1}, \Theta_2, \mathcal{M}_2) \tag{2.1}$$

where $w_1 \in [0, 1]$ is the model weight on $\mathcal{M}_1$.

Waggoner and Zha (2012) extend the approach of Geweke and Amisano (2011) and allow the model weights to vary over time. They replace w_1 in equation (2.1) by $w_{1,s_t} \in [0, 1]$ where s_t takes either 1 or 2 following a first-order two-state Markov process with constant transition probabilities

$$q_{ij} = \Pr[s_t = j|s_{t-1} = i], \; i, j = 1, 2$$

In doing so this they consider the case where the relative importance of each of the prediction models can change over time. The resulting predictive density conditioned on the regime s_t is given by

$$w_{1,s_t} \times p(\mathbf{y}_t|Y_{t-1}, \Theta_1, \mathcal{M}_1) + (1 - w_{1,s_t}) \times p(\mathbf{y}_t|Y_{t-1}, \Theta_2, \mathcal{M}_2).$$

By letting the model-specific parameters $\Theta = \{\Theta_1, \Theta_2\}$, transition probabilities $Q = \{q_{11}, q_{22}\}$, and the regime-dependent model weight $w = \{w_{1,1}, w_{1,2}\}$ the likelihood can be constructed as

$$\log p(Y_T|\Theta, Q, w) = \sum_{t=1}^{T} \log p(\mathbf{y}_t|Y_{t-1}, \Theta, Q, w)$$

where the regime s_t is integrated out because it is never observed by econometricians. For more details on the likelihood computation, refer to Appendix A.

Although we follow the proposed approaches in Geweke and Amisano (2012) and Waggoner and Zha (2012), our study differs in several dimensions. First, we concentrate on yield curve forecasting while they forecast macroeconomic variables such as the GDP growth rate and inflation. Second, in our work the model-specific parameters, the model weights, and the transition probabilities are estimated simultaneously, not sequentially. As Waggoner and Zha (2012) and Del Negro et al. (2016) point out, the joint estimation of model parameters and model weights is conceptually desirable. However, it is numerically challenging because the likelihood is high-dimensional and non-linear. Due to the efficient Bayesian MCMC sample method suggested by Chib and Ergashev (2009) and Chib and Kang (2016), we are able to deal with the numerical problem and estimate them jointly. The key idea of the posterior sampling is to approximate the full conditional distributions by a Student-t distribution. The mean and scale matrix are obtained from a stochastic optimization in order to deal with the irregular posterior surface. In addition, the number of blocks and their components are randomized in every MCMC cycle, which helps improve efficiency of the sample when the model is high-dimensional and severely nonlinear to the parameters. Third, most importantly, both short- and long-term forecasts are produced and used for model comparison whereas they assess the predictive performance of pooled models based on the log predictive score, which is a good measurement of one-step-ahead predictive accuracy.

3 Models

In this section we briefly discuss the three individual yield curve prediction models commonly used for yield curve prediction. Then, we introduce our pooled models as

alternative prediction models.

3.1 Individual Yield Curve Prediction Models

3.1.1 Dynamic Nelson-Siegel Model

We begin by describing the three-factor dynamic Nelson-Siegel model (Diebold and Li (2006)). In the DNS model, the bond yields are specified as a linear function of the vector of three exogenous latent factors $\mathbf{x}_t$

$$\mathbf{y}_t|\mathbf{x}_t, \mathbf{\Sigma}_{NS} \sim \mathcal{N}\left(\mathbf{\Lambda}\mathbf{x}_t, \mathbf{\Sigma}_{NS}\right) \tag{3.1}$$

where $\mathcal{N}(.,.)$ denotes the multivariate normal distribution, the measurement error variance matrix $\mathbf{\Sigma}_{NS}$ is diagonal, and λ is a decay parameter,

$$\mathbf{\Lambda} = \begin{pmatrix} 1 & \frac{1-e^{-\tau_1\lambda}}{\tau_1\lambda} & \frac{1-e^{-\tau_1\lambda}}{\tau_1\lambda} - e^{-\tau_1\lambda} \\ 1 & \frac{1-e^{-\tau_2\lambda}}{\tau_2\lambda} & \frac{1-e^{-\tau_2\lambda}}{\tau_2\lambda} - e^{-\tau_2\lambda} \\ \vdots & \vdots & \vdots \\ 1 & \frac{1-e^{-\tau_N\lambda}}{\tau_N\lambda} & \frac{1-e^{-\tau_N\lambda}}{\tau_N\lambda} - e^{-\tau_N\lambda} \end{pmatrix}, \tag{3.2}$$

$$\text{and } \mathbf{x}_t = \begin{pmatrix} \mathbf{x}_t^L & \mathbf{x}_t^S & \mathbf{x}_t^C \end{pmatrix}'. \tag{3.3}$$

The vector of the dynamic factors $\mathbf{x}_t$ is assumed to follow the first-order stationary vector autoregressive (VAR) process,

$$\mathbf{x}_t|\mathbf{x}_{t-1}, \kappa, \phi, \Omega_{NS} \sim \mathcal{N}\left(\kappa + \phi\mathbf{x}_{t-1}, \Omega_{NS}\right). \tag{3.4}$$

For stationarity, the absolute of all eigen values of $\phi : 3 \times 3$ is constrained to be less than 1, and $\mathbf{x_0}$ is assumed to be generated from the unconditional distribution of $\mathbf{x}_t$. Because of the functional form of the factor loadings $\mathbf{\Lambda}$, the latent dynamic factors, $\mathbf{x}_t^L$, $\mathbf{x}_t^S$ and $\mathbf{x}_t^C$ are identified and interpreted as level, slope, and curvature effects, respectively. The coefficient λ, referred to as the decay parameter, determines the exponential decay rate of the factor loadings and is fixed at 0.0607 as in Diebold and Li (2006).

Then, the set of the parameters to be estimated in the DNS model is

$$\Theta_{NS} = \{\kappa, \phi, \Omega_{NS} = V_{NS}\Gamma_{NS}V_{NS}, \mathbf{\Sigma}_{NS}\}$$

where $V_{NS} : 3 \times 3$ and $\Gamma_{NS} : 3 \times 3$ are the factor shock volatility and correlation matrices, respectively.

Finally, because the equations (3.1) and (3.4) are a standard state-space representation, the resulting conditional density of $\mathbf{y}_t$ at each time point

$$p(\mathbf{y}_t|Y_{t-1}, \Theta_{NS}, \mathcal{M}_{NS}) \tag{3.5}$$

can be easily obtained from the usual Kalman filtering procedure.

3.1.2 Arbitrage-free Nelson-Siegel Model

Bond Prices The arbitrage-free Nelson-Siegel (AFNS) model is a theoretical bond pricing approach based on partial equilibrium, while the DNS model is a purely statistical approach. Satisfying the arbitrage-free condition, the bond prices are endogenously determined by economic agents who know the model parameters.

Let $P_t(\tau)$ denote the price of the bond at time t that matures in period $(t + \tau)$. Following Duffie and Kan (1996), we assume that $P_t(\tau)$ is an exponential affine function of the vector of three-dimensional factors $\mathbf{f}_t$ taking the form

$$P_t(\tau) = \exp(-\tau y_t(\tau)) \tag{3.6}$$

where $y_t(\tau)$ is the continuously compounded yield given by

$$y_t(\tau) = -\frac{\log P_t(\tau)}{\tau} = a(\tau) + b(\tau)'\mathbf{f}_t,$$

$a(\tau)$ is a scalar, and $b(\tau)$ is a 3×1 vector, both depending on τ. These coefficients are endogenously determined by the no-arbitrage condition given certain assumptions for the dynamic evolution of the factors and the stochastic discount factor.

To impose the no-arbitrage condition

$$P_t(\tau) = \mathbb{E}[M_{t,t+1}P_{t+1}(\tau - 1)|\mathbf{f}_t]$$

given the stochastic discount factor (SDF), $M_{t,t+1}$, we solve the risk-neutral pricing equation for these coefficients. To do this, we specify the factor process and the SDF. The distribution of $\mathbf{f}_t$, conditioned on $\mathbf{f}_{t-1}$, is determined by a Gaussian mean-reverting first-order autoregression

$$\mathbf{f}_t = G\mathbf{f}_{t-1} + \boldsymbol{\eta}_t, \quad \boldsymbol{\eta}_t \sim \mathcal{N}(\mathbf{0}, \Omega_{AF}) \tag{3.7}$$

where $G : 3 \times 3$ is a vector auto-regressive (VAR) coefficient matrix. In the sequel, we express $\boldsymbol{\eta}_t$ in terms of a vector of i.i.d. standard normal variables $\boldsymbol{\omega}_t$ as $\boldsymbol{\eta}_t = \mathbf{L}\boldsymbol{\omega}_t$ where $\mathbf{L}$ is the lower-triangular Cholesky decomposition of Ω_{AF}.

We complete our modeling by assuming that the SDF $M_{t,t+1}$ that converts a time $(t+1)$ payoff into a payoff at time t is given by

$$M_{t,t+1} = \mathsf{exp}\left(-r_t - \frac{1}{2}\boldsymbol{\gamma}_t'\boldsymbol{\gamma}_t - \boldsymbol{\gamma}_t'\boldsymbol{\omega}_{t+1}\right) \tag{3.8}$$

where r_t is the short-rate, $\boldsymbol{\gamma}_t$ is the vector of time-varying market prices of factor risks, and $\boldsymbol{\omega}_{t+1}$ is the i.i.d. vector of factor shocks at time $t+1$. We suppose that the short rate and the market price of factor risk are both affine in the factors

$$r_t = \delta + \boldsymbol{\beta}'\mathbf{f}_t, \tag{3.9}$$

$$\boldsymbol{\gamma}_t = \bar{\boldsymbol{\gamma}} + \Phi\mathbf{f}_t. \tag{3.10}$$

Given the assumptions above, we find the solutions for $a(\tau)$ and $b(\tau)$ in terms of the structural parameters by using the method of undetermined coefficients. Incorporating the assumptions for the factor and SDF process into the risk-neutral pricing formula yields the following recursive system for the unknown functions

$$\begin{aligned} a(\tau) &= \delta/\tau + a(\tau-1) - b(\tau-1)'\mathbf{L}\bar{\boldsymbol{\gamma}} - \frac{\tau}{2}b(\tau-1)'\Omega_{AF}b(\tau-1) \\ b(\tau) &= \boldsymbol{\beta}/\tau + (G - \mathbf{L}\Phi)'b(\tau-1) \end{aligned} \tag{3.11}$$

where $G^Q = G - \mathbf{L}\Phi$ and τ runs over the positive integers. These recursions are initialized by setting $a(0) = 0$ and $b(0) = 0_{3\times 1}$.

Econometric Model Now we express the AFNS model as an econometric model for estimation. First, we let $\mathbf{a}$ and $\mathbf{b}$ be the corresponding intercept and factor loadings for $\mathbf{y}_t$ obtained from the recursive equations in (3.11).

$$\begin{aligned} \mathbf{a} &= \begin{pmatrix} a(\tau_1) & a(\tau_2) & \cdots & a(\tau_N) \end{pmatrix}' : N \times 1 \\ \mathbf{b} &= \begin{pmatrix} b(\tau_1) & b(\tau_2) & \cdots & b(\tau_N) \end{pmatrix}' : N \times 3 \end{aligned} \tag{3.12}$$

For computational convenience, we follow Bansal and Zhou (2002) and Chib and Kang (2013) and assume that three basis bonds (the three-month, three-year, and ten-year) are

observed without errors. These three maturities are the first, fifth, and eighth maturities in our dataset. This implies that there is a one-to-one mapping between the three latent factors and basis yields such that

$$\begin{aligned} \mathbf{y}_t^B &= \mathbf{a}_B + \mathbf{b}_B \mathbf{f}_t \\ \text{or } \mathbf{f}_t &= (\mathbf{b}_B)^{-1} \times (\mathbf{y}_t^B - \mathbf{a}_B) \end{aligned}$$

where

$$\begin{aligned} \mathbf{y}_t^B &= \begin{pmatrix} y(\tau_1) & y(\tau_5) & y(\tau_8) \end{pmatrix}', \\ \mathbf{a}_B &= \begin{pmatrix} a(\tau_1) & a(\tau_5) & a(\tau_8) \end{pmatrix}' : 3 \times 1, \\ \text{and } \mathbf{b}_B &= \begin{pmatrix} b(\tau_1) & b(\tau_5) & b(\tau_8) \end{pmatrix}' : 3 \times 3. \end{aligned}$$

Let $\mathbf{a}_{NB}$ and $\mathbf{b}_{NB}$ denote the intercept term and factor loadings corresponding to the non-basis yields. The non-basis yields, denoted by $\mathbf{y}_t^{NB}$, are observed with errors,

$$\mathbf{y}_t^{NB} | \mathbf{a}_{NB}, \mathbf{b}_{NB}, \mathbf{f}_t \sim \mathcal{N}(\mathbf{a}_{NB} + \mathbf{b}_{NB}\mathbf{f}_t, \mathbf{\Sigma}_{AF}).$$

where $\mathbf{\Sigma}_{AF} : 5 \times 5$ is a diagonal matrix.

Identifying Restrictions For factor identification we impose two restrictions. First, the matrix $\boldsymbol{G}^Q$ has the form

$$\boldsymbol{G}^Q = \begin{bmatrix} 1 & 0 & 0 \\ 0 & \exp(-g^Q) & g^Q \exp(-g^Q) \\ 0 & 0 & \exp(-g^Q) \end{bmatrix}. \tag{3.13}$$

Second, the vector $\boldsymbol{\beta}$ is constrained to be

$$\boldsymbol{\beta} = (1, 1, 0,)'.$$

As shown in Niu and Zeng (2012), because of these restrictions, $\mathbf{b}$ in equation (3.12) reduces to exactly the form of the dynamic Nelson-Siegel factor loading structure $\mathbf{\Lambda}$. Therefore, the factors $\mathbf{f}_t$ are also identified as the level, slope, and curvature effects as in the DNS model.

Unlike the DNS model, however, the structural parameters in the AFNS model determining the intercept term, factor loadings, factor persistence, and factor volatilities

are jointly estimated. At the same time, in the DNS model, the intercept term and factor loadings are fixed, and Θ_{NS} collects the parameters in the factor process and measurement error variances.

Suppose that $V_{AF} : 3 \times 3$ is the factor shock volatility and $\Gamma_{AF} : 3 \times 3$ is the factor shock correlation matrix. Following Dai, Singleton, and Yang (2007) we fix δ at the sample mean of the short rate because the short rate is highly persistent and δ tends to be inefficiently estimated. Finally, the set of parameters in the AFNS model to be estimated is

$$\Theta_{AF} = \{G, g^Q, \Omega_{AF} = V_{AF}\Gamma_{AF}V_{AF}, \mathbf{\Sigma}_{AF}\}.$$

The resulting conditional density of $\mathbf{y}_t$ is obtained by

$$\begin{aligned} p(\mathbf{y}_t|Y_{t-1}, \Theta_{AF}, \mathcal{M}_{AF}) &= p(\mathbf{y}_t^{NB}|\mathbf{y}_t^B, \Theta_{AF}, \mathcal{M}_{AF}) \times p(\mathbf{y}_t^B|\mathbf{y}_{t-1}^B, \Theta_{AF}, \mathcal{M}_{AF}) \qquad (3.14) \\ &= \mathcal{N}(\mathbf{y}_t^{NB}|\mathbf{a}_{NB} + \mathbf{b}_{NB}\mathbf{f}_t, \mathbf{\Sigma}_{AF}) \times \mathcal{N}(\mathbf{f}_t|G\mathbf{f}_{t-1}, \Omega_{AF}) \times |\mathbf{b}_B^{-1}| \end{aligned}$$

where $\mathbf{f}_t = (\mathbf{b}_B)^{-1} \times \left(\mathbf{y}_t^B - \mathbf{a}_B\right)$, and $\mathcal{N}(x|m, V)$ denotes the multivariate normal density of x with mean m and variance-covariance V.

3.1.3 Random-Walk Model

The third individual prediction model contained in our pool is the RW,

$$\mathbf{y}_t|\mathbf{y}_{t-1}, \mathbf{\Sigma}_{RW} \sim \mathcal{N}(\mathbf{y}_{t-1}, \mathbf{\Sigma}_{RW}) \qquad (3.15)$$

where $\Theta_{RW} = \mathbf{\Sigma}_{RW}$ is an $N \times N$ diagonal matrix. The conditional density of $\mathbf{y}_t$ is simply

$$p(\mathbf{y}_t|Y_{t-1}, \Theta_{RW}, \mathcal{M}_{RW}) = \mathcal{N}(\mathbf{y}_t|\mathbf{y}_{t-1}, \mathbf{\Sigma}_{RW}). \qquad (3.16)$$

As demonstrated by Altavilla, Giacomini, and Ragusa (2014) and Diebold and Li (2006), outperforming the random walk in terms of out-of-sample yield curve forecasting is challenging, and it is often used as a benchmark in prediction ability comparisons. Therefore, we include the RW in our pool.

3.2 Pooled Models

Diebold and Li (2006) show that overall DNS produces better forecast accuracy in out-of-sample predictions than Duffie's (2002) best essentially affine model, although the RW

forecasts better at short forecast horizons. Then the Bayesian model-averaging method based on the Bayes factor would yield nearly one weight on the DNS model excluding the AFNS and RW models. Nevertheless, all these prediction models have been commonly used for forecasting the term structure of interest rates, and none of them consistently outperforms the others at all maturities and forecast horizons. One potential reason is that the alternative models are somewhat misspecified, which indicates that model uncertainty is substantial.

Given the potential model misspecification of the alternative models, we investigate whether combining the multiple models in a linear form helps improve predictive accuracy. Table 1 presents 15 competing pooled models with various combinations. We consider the individual models. Additionally, the linear combinations of two and three of the alternatives are used for prediction. The model weights can be either constant or time-varying. For the pooled models with constant weights, the weights are estimated or equally given. For instance, the NS-AF-RW-*Const* is the pooled model of the DNS, AFNS and RW with a constant weight. The NS-AF-RW-*MS* is the pooled model with Markov regime-switching weights, in which the model weights vary over time according to the Markov process. In NS-AF-RW-*Equal*, each of the model weights is fixed at a third.

4 Posterior Simulation

This section discusses the posterior sampling scheme for the most general model among the competing models, the NS-AF-RW-*MS* model. The others can be estimated as special cases of the NS-AF-RW-*MS* model. In the Bayesian context our pooled model with Markov regime-switching weights is the joint prior distribution of the yield curves ($\mathbf{Y} = \{\mathbf{y}_t\}_{t=1}^{T}$), the regime indicators ($\mathbf{S} = \{s_t\}_{t=1}^{T}$), the continuous latent variables ($\mathbf{X} = \{\mathbf{x}_t\}_{t=1,2,..,T}$ and $\mathbf{F} = \{\mathbf{f}_t\}_{t=1,2,..,T}$)), and the model parameters ($\boldsymbol{\psi}$= $\{\Theta_{NS}$, Θ_{AF}, Θ_{RW}, Q, $w\}$). Given the joint density, our objective is to simulate the posterior distribution of $(\boldsymbol{\psi}, \mathbf{X}, \mathbf{F}, \mathbf{S})$ conditioned on the observed yield curves $\mathbf{Y}$**.** Its density has the form

$$\pi\left(\boldsymbol{\psi}, \mathbf{X}, \mathbf{F}, \mathbf{S}|\mathbf{Y}\right) \propto f\left(\mathbf{Y}|\boldsymbol{\psi}, \mathbf{X}, \mathbf{F}, \mathbf{S}\right) \times f\left(\mathbf{X}, \mathbf{F}|\boldsymbol{\psi}\right) \times p\left(\mathbf{S}|\boldsymbol{\psi}\right) \times \pi(\boldsymbol{\psi}) \qquad (4.1)$$

where $\pi(\boldsymbol{\psi})$ is the prior density of the parameters and $p(\mathbf{S}|\boldsymbol{\psi})$ is the prior density function for regime-indicators given the parameters; it is specified as the discrete two-state Markov switching process. $f(\mathbf{X}, \mathbf{F}|\mathbf{S}, \boldsymbol{\psi})$ is the prior density of the factors and $f(\mathbf{Y}|\boldsymbol{\psi}, \mathbf{X}, \mathbf{F}, \mathbf{S})$ is the joint conditional density of the observed data.

4.1 Prior

The prior for $(\Theta_{NS}, \Theta_{AF})$ that we give in the paper is set up to reflect the a priori belief that the yield curve is gently upward sloping and concave on average. Particularly, the prior of Θ_{AF} should be chosen very carefully because the bond yields are highly nonlinear to the parameters, and the likelihood surface of the AFNS tends to be irregular. The irregularity of the posterior surface can be more serious or mitigated depending on the choice of the prior. We use the prior used in the work of Chib and Kang (2016). As Chib and Ergashev (2009) suggest, Chib and Kang (2016) arrive at the prior by prior simulation technique, sampling parameters from the assumed prior, then sampling the data given the parameters repeating this process many times until the mean of the resulting prior-implied unconditional distribution of the yield curve is mildly upward sloping and concave. Chib and Ergashev (2009) and Chib and Kang (2016) document that this simulation-based prior can smooth out the many local modes of the likelihood surface.

Additionally, we assume that ϕ and G are diagonal since this restriction helps improve the predictive accuracy and reduces the computational burden (Christensen et al. (2011)). Table 2 summarizes our prior.

For regime identification, we impose a restriction that the weight on the DNS model $\mathcal{M}_{NS}$, denoted by w_{NS,s_t}, should be higher in regime 2 than in regime 1

$$0 < w_{NS,s_t=1} < w_{NS,s_t=2} < 1 \text{ and } 0 < w_{NS,s_t} + w_{AF,,s_t} < 1$$

where w_{AF,s_t} is the weight on the AFNS model. For the *MS*-AF-RW model, the restriction is replaced by

$$0 < w_{AF,s_t=1} < w_{AF,s_t=2} < 1.$$

All the restrictions including those of factor identification and regime identification are imposed through the prior.

4.2 MCMC Sampling

Because the joint posterior distribution in equation (4.1) is not analytically tractable, we rely on an MCMC simulation method and sample the parameters, factors, regimes, and predictive yield curves recursively from the joint posterior distribution as follows:

Algorithm 1: MCMC sampling

- Step 1: Sample $\Theta_{NS}, \Theta_{AF}, \Theta_{RW}, w|\mathbf{Y}$,$Q$
  - Step 1(a): Sample $\Theta_{NS}, \Theta_{AF}, \Theta_{RW}, w|\mathbf{Y}$,$Q$
  - Step 1(b): Sample $Q|\mathbf{Y}, \mathbf{S}$,$\Theta_{NS}, \Theta_{AF}, \Theta_{RW}, w$
- Step 2: Sample $\mathbf{S}|\mathbf{Y}$,$\boldsymbol{\psi}$
- Step 3: Sample $\mathbf{X}|\mathbf{Y}$,$\boldsymbol{\psi}$ and $\mathbf{F}|\mathbf{Y}$,$\boldsymbol{\psi}$
- Step 4: Sample $\{\mathbf{y}_{T+h}\}_{h=1}^{H}|\mathbf{Y}, \mathbf{X}, \mathbf{F}, \mathbf{S}$,$\boldsymbol{\psi}$

More details on MCMC sampling in each step can be found in Appendix B.

5 Predictive Accuracy Measures

We evaluate predictive accuracy using two measures. One is the posterior predictive criterion (PPC) of Gelfand and Ghosh (1998), which is often used for density forecast evaluation. The other measure is the root mean squared error (RMSE), which is a popular measure of point forecast accuracy.[3]

[3]Throughout the paper we evaluate the predictive accuracy of multiple individual bond yields instead of the yield curve in order to see maturity-specific prediction performance of the prediction models and compare the results with those in the literature. The predictive accuracy of the yield curve can be measured by the log predictive likelihood as in Kang (2015).

5.0.1 Posterior Predictive Criterion

We follow Zantedeschi et al. (2011) and Chib and Kang (2013) and evaluate the predictive accuracy of the density forecasts by using the posterior predictive criterion (PPC) of Gelfand and Ghosh (1998). Suppose that $y^o_{T+h}(\tau)$ is the realized τ-month bond yield, and $\mathbb{E}\left(y_{T+h}(\tau)|\mathbf{Y}\right)$ is the posterior mean of $y_{T+h}(\tau)$. Given each pooled model and in-sample data $\mathbf{Y}$, the PPC for the h-month-ahead posterior predictive density of $\tau-$period bond yield, $\mathsf{PPC}_{\mathbf{Y}}(\tau, h)$ is computed as

$$\mathsf{PPC}_{\mathbf{Y}}(\tau, h) = \mathsf{D}_{\mathbf{Y}}(\tau, h) + \mathsf{W}_{\mathbf{Y}}(\tau, h)$$

where

$$\mathsf{D}_{\mathbf{Y}}(\tau, h) = \mathsf{Var}\left(y_{T+h}(\tau)|\mathbf{Y}\right)$$

and

$$\mathsf{W}_{\mathbf{Y}}(\tau, h) = \left[y^o_{T+h}(\tau) - \mathbb{E}\left(y_{T+h}(\tau)|\mathbf{Y}\right)\right]^2$$

The term $\mathsf{D}_{\mathbf{Y}}(\tau, h)$ is the posterior variance of the predictive yield, which is large when the model has too many restrictions or redundant parameters. The term $\mathsf{W}_{\mathbf{Y}}(\tau, h)$ is the squared errors and evaluates the predictive goodness-of-fit. Let T_H denote the number of the out-of-sample datasets. Then, the $\mathsf{PPC}(\tau, h)$ is obtained as the average of $\mathsf{PPC}_{\mathbf{Y}}(\tau, h)$ over the 108(=T_H) out-of-samples.

$$\mathsf{PPC}(\tau, h) = \frac{1}{T_H} \sum_{\mathbf{Y}} \mathsf{PPC}_{\mathbf{Y}}(\tau, h)$$

5.0.2 Root Mean Squared Error

The RMSE of the h-month-ahead bond yield with τ-month to maturity, denoted by $RMSE(\tau, h)$, is given by

$$RMSE(\tau, h) = \sqrt{\frac{1}{T_H} \sum_{\mathbf{Y}} \left[y^o_{T+h}(\tau) - \mathbb{E}\left(y_{T+h}(\tau)|\mathbf{Y}\right)\right]^2}.$$

By definition, smaller values of PPC and RMSE are preferable.

6 Empirical Results

In this section, we evaluate and compare the out-of-sample forecasting performance of the pooled models. We especially concentrate on the predictive gain of pooling the individual yield curve prediction models.

Our data comprise monthly yields on U.S. government bonds. The time span is from February 1994 to December 2013. The set of maturities in months is {3, 6, 12, 24, 36, 60, 84, 120}. The data are obtained from the Federal Reserve Bank of St. Louis economic data.

For a model comparison, we calculate PPC and RMSE values from a rolling window estimation. The window size is 120 months, and the forecast horizon is one through twelve months. The first out-of-sample period is February 2004 to January 2005, and the corresponding in-sample period is February 1994 to January 2004. We simulate the predictive yield curves and compute the squared errors and $\mathsf{PPC}_{\mathbf{Y}}$. Then, we move forward the in-sample and out-of-sample by one month and compute the squared errors and $\mathsf{PPC}_{\mathbf{Y}}$. This procedure is repeated 108 times where the last out-of-sample period is January 2013 to December 2013. Finally, we obtain 108 squared errors and $\mathsf{PPC}_{\mathbf{Y}}$s for each pair of maturities and forecast horizons. Using these results, we are able to compute and compare the PPCs and RMSEs of the pooled models with those of the individual models. The in-sample and out-of-sample pairs are shown in Table 3.

6.1 PPC Comparison

Table 4 presents the best models based on the PPC for each of 96 pairs of maturities and forecast horizons (12 forecast horizons times eight maturities). For easier reference, we use shorter model specification indices: "N" stands for the DNS, "A" for the AFNS, and "R" for the RW. The subscript "E" stands for the equal weights, "C" for the constant weights, and "M" for the Markov-switching weights. For example, "NR_E" in Table 4 indicates the pooled model of DNS and RW with the equal-weight model (i.e., NS-RW-*Equal*).

Table 4 shows that the best models are pooled models. Particularly, the equal-weight

NS-RW model, NS-RW-*Equal*, outperforms the other models for the maturities of three months through three years regardless of the forecast horizon. For the seven-year bond yield, the NS-RW-*Equal* forecasts best at all the forecast horizons except for the one-month-ahead forecast. Additionally, pooling all individual models with equal weights is found to improve the predictive accuracy of five- and ten-year bond yields.

Tables 5 and 6 report the PPCs for the maturities at 1-, 3-, 6-, and 12-month-ahead horizons to show the relative performance of the alternative models. The PPCs are normalized by that of the RW model for each maturity. The values larger than one favor the RW model. Bold entries indicate the best prediction models for each pair of maturities and forecast horizons.

There are three important implications from the PPC comparison. First, as shown in Tables 5 and 6, the predictive gain from the pooling method is remarkable. The NS-RW-*Equal* consistently outperforms the three individual models across all maturities and forecast horizons by a substantial margin. Meanwhile, the Bayesian model averaging tends to pick one of the three individual models. Either the DNS or RW model is typically selected, but their density forecasting performance is found to be worse than that of the pooled model of the DNS and RW.

It should be noted that pooling individual models does not guarantee better density forecasts than selecting one of the individual models. As Tables 5 and 6 demonstrate, many pooled models produce less accurate forecasts than the DNS or RW model. The more models included in the pool, the greater the number of parameters that need to be estimated. Because the information contained in the data is limited and the models in the pool share the information, prediction can be inefficient, which leads to a very large posterior variance of the predictive yields.

Second, although the RW model is not the best prediction model for density forecasting, all the best model combinations include the RW model in the pool. Therefore, the RW plays an essential role in improving density forecasting. Third, the theoretical model, the AFNS, can help produce more accurate density forecasts of long-term bond yields, and this model should not be excluded from the pool. In particular, for five-year bond yield prediction, the AFNS is operative at all horizons. This finding is meaningful

because the AFNS has been less popular than the DNS and RW models in yield curve prediction.

It is interesting that the best pooled models have equal model weights. Estimating the weights, which either are constant or follow the Markov process, can improve in-sample-fit. At the same time, however, it causes inefficiency. This inefficiency has already been noted in the literature, for instance by Smith and Wallis (2009), Stock and Watson (2004), and Winkler and Clemen (1992).

6.2 RMSE Comparison

We move to the point forecasting evaluation of the pooling method. For each pair of the maturities and forecast horizons, we calculate the $RMSE(\tau, h)$ and choose the best prediction models producing the smallest RMSE value among the competing models. Table 7 presents the best models for each maturity across forecast horizons. Tables 8 and 9 report the RMSEs for the maturities at 1-, 3-, 6-, and 12-month-ahead horizons to show the relative prediction ability of the alternative models. Like in the PPC comparison, the RMSEs are normalized by that of the RW model. Bold entries indicate the best prediction performance.

Two important findings emerge from the tables. First, in terms of the point prediction, the RW model outperforms the other models in 73 of 96 cases in contrast to the results from the PPCs. Particularly, the RW produces the most accurate point forecasts of 3-, 24-, 36-, 60-, and 84-month bond yields at all forecast horizons.

Second, the pooled model, NS-RW-*MS* forecasts best for six-month bond yields at long forecast horizons. In addition, the NS-AF-*Const* is superior in short-term forecasting of the 10-year bond yield. As shown in Tables 8 and 9, however, the differences between the RMSEs of the two pooled models and the RW model are not substantial. Therefore, in terms of point forecasts the predictive gain from pooling various yield curve models does not seem remarkable.

6.3 Further Discussion

6.3.1 Forecasting Performance before and after the Crisis

For a robustness check, we split the 108 out-of-sample periods into two subsamples and evaluate the pooling method based on the PPC and RMSE values. The first and second 54 out-of-sample periods range from January 2004 to June 2008 and from July 2008 to December 2012, which correspond to the pre-crisis and post-crisis periods, respectively. Tables 10 and 11 report the best models that achieve the smallest PPC and RMSE values for the two out-of-sample periods.

As shown in the tables, the best models are different across out-of-sample periods. Before the crisis the all individual models operate. The AFNS model is especially included in most of the best pools, and it performs well even in the point forecasting. Thus, during the normal period the theoretical model appears reliable. Meanwhile, after the crisis, the RW seems to be most important as an individual model and for model combination. The bigger role of the RW model after the crisis can be attributed to the fact that the RW has an advantage in considering the possibility of a structural change in the U.S. yield curve dynamics.

On the other hand, the results from the recent 54 out-of-sample forecast periods are consistent with those from the full forecast periods. This implies that the results from the recent out-of-sample periods dominate those from the first out-of-sample periods.

6.3.2 Model Weights and Posterior Probability of Regimes

Finally, we discuss the estimates of the model weights using the full sample from February 1994 to December 2013. These estimates can be a measure of the relative importance of each individual model in the pooled models. Table 12 presents the estimated weights for the constant-weight model. We find that the DNS model has a higher weight in general, and the RW model has a lower weight during the full sample period.

However, the model weights do not seem to be constant over time. Table 13 presents the estimated Markov-switching weights, and Figure 1 plots the posterior probabilities of regime 2. First, the model weights are strongly regime-dependent, and the regime changes are drastic over time. As a result, the regimes seem to be well-identified. Recall

that the model-specific parameters and model weights are jointly estimated in our work. For this reason, the parameters in a model are heavily determined by the observations in the regime when the model has a large weight.

More importantly, the role of the RW model in the pooled models becomes more important after the recent crisis. For instance, in the case of the NS-AF-RW-*MS,* the weights on the DNS and RW models in regime 1 are 0.219 and 0.429, respectively. Meanwhile, the weights are 0.752 and 0.133 in regime 2. As Figure 1 shows, the posterior probability of regime 2 has been persistent but decreased drastically around 2008. Hence, the predictive ability of the DNS model was superior before the recent financial crisis, but the RW model was dominant after the crisis. As mentioned earlier, this is because the yield curve dynamics may have undergone a structural change around the crisis and is detected by the RW process. Table 13 and Figure 1 report the NS-RW-*MS* and AF-RW-*MS* model estimation results and confirm the increasing importance of the RW model.

One natural question is why dynamic pooling performs worse than static pooling despite the obvious regime changes in the model weights. This is because the timing of the regime changes is too close to the end of the sample, and the observations during regime 1 are not informative enough. As a result, the inefficiency caused by estimating the transition probabilities and model weights and forecasting the future regimes makes the dynamic prediction pools perform poorly. For an extended period of time, the pooled model with the Markov-switching weights may generate more accurate forecasts when the regime shift is permanent or very persistent. However, if the regime changes are frequent like in Figure 1 (b), the dynamic pooling approach is not desirable.

7 Conclusion

In this paper we examine whether the pooling method can help improve the accuracy of yield forecasts. The pool of models includes the dynamic Nelson-Siegel model, the arbitrage-free Nelson-Siegel model, and the random walk model. We combine these potentially misspecified models in a linear form suggested by Geweke and Amisano (2011),

Geweke and Amisano (2012), and Waggoner and Zha (2012). We evaluate the out-of-sample forecasts of the pooled models based on the PPC and RMSE. The empirical results of the PPC comparison demonstrate that the pooled model of the DNS and RW with equal weights produces accurate density forecasts dominating the three individual models at all maturities and forecast horizons, whereas the predictive gain from the pooling method does not seem to be substantial in the point forecasts.

The most important implication of our empirical findings is that despite the higher computational cost, the pooling method is worth trying when multiple bond yield prediction models compete. However, we do not argue that our pooled model is the best model because another pooled model of different individual models can exhibit better forecasting performance. The DNS and AFNS models with macroeconomic factors or regime-switching yield curve models could be included in the pool. In addition, it would be interesting to examine various approaches to averaging bond yield forecasts and compare their performance as in Clark and McCracken (2010) and De Pooter, Ravazzolo, and Van Dijk (2010). We leave this as future work.

References

Almeida, C. and Vicenteb, J. (2008), "The role of no-arbitrage on forecasting: Lessons from a parametric term structure model," *Journal of Banking and Finance*, 32(12), 2695–2705.

Altavilla, C., Giacomini, R., and Ragusa, G. (2014), "Anchoring the Yield Curve using Survey Expectations?" *European Central Bank Working Paper 1632*, 1–28.

Bansal, R. and Zhou, H. (2002), "Term structure of interest rates with regime shifts," *Journal of Finance*, 57(5), 463–473.

Carrieroa, A. and Giacomini, R. (2011), "How useful are no-arbitrage restrictions for forecasting the term structure of interest rates?" *Journal of Econometrics*, 164(1), 21–34.

Carter, C. and Kohn, R. (1994), "On Gibbs sampling for state space models," *Biometrika*, 81, 541–53.

Chib, S. (1998), "Estimation and comparison of multiple change-point models," *Journal of Econometrics*, 86, 221–241.

Chib, S. and Ergashev, B. (2009), "Analysis of multi-factor affine yield curve Models," *Journal of the American Statistical Association*, 104, 1324–1337.

Chib, S. and Kang, K. H. (2013), "Change Points in Affine Arbitrage-free Term Structure Models," *Journal of Financial Econometrics*, 11(2), 302–334.

— (2016), "An Efficient Posterior Sampling in Gaussian Affine Term Structure Models," *Manuscript*, 1–28.

Chib, S. and Ramamurthy, S. (2010), "Tailored Randomized-block MCMC Methods with Application to DSGE Models," *Journal of Econometrics*, 155, 19–38.

Christensen, J. H. E., Diebold, F. X., and Rudebusch, G. D. (2011), "The affine arbitrage-free class of Nelson-Siegel term structure models," *Journal of Econometrics*, 164, 4–20.

Clark, T. E. and McCracken, M. W. (2010), "Averaging forecasts from VARs with uncertain instabilities," *Journal of Applied Econometrics*, 25(1), 5–29.

Dai, Q., Singleton, K. J., and Yang, W. (2007), "Regime shifts in a dynamic term structure model of U.S. treasury bond yields," *Review of Financial Studies*, 20, 1669–1706.

De Pooter, M. (2007), "Examining the Nelson-Siegel Class of Term Structure Models," *Tinbergen Institute Discussion Paper*.

De Pooter, M., Ravazzolo, F., and Van Dijk, D. J. C. (2010), "Term Structure Forecasting Using Macro Factors and Forecast Combination," *FRB International Finance Discussion Paper No. 993*, 1–49.

Del Negro, M., Hasegawa, R. B., and Schorfheide, F. (2016), "Dynamic Prediction Pools: An Investigation of Financial Frictions and Forecasting Performance," *Journal of Econometrics*, in press.

Diebold, F. X. and Li, C. L. (2006), "Forecasting the term structure of government bond yields," *Journal of Econometrics*, 130, 337–364.

Duffie, G. (2002), "Term premia and interest rate forecasts in affine models," *Journal of Finance*, 57, 405–43.

Duffie, G. and Kan, R. (1996), "A yield-factor model of interest rates," *Mathematical Finance*, 6, 379–406.

Gelfand, A. E. and Ghosh, S. K. (1998), "Model choice: A minimum posterior predictive loss approach," *Biometrika*, 85, 1–11.

Geweke, J. and Amisano, G. (2011), "Optimal prediction pools," *Journal of Econometrics*, 164(1), 130–141.

— (2012), "Prediction with Misspecified Models," *American Economic Review*, 102(3), 482–486.

Kang, K. H. (2015), "Predictive Density Simulation of Yield Curves with a Zero Lower Bound," *Journal of Empirical Finance*, 51–66.

Moench, E. (2008), "Forecasting the yield curve in a data-rich environment: A no-arbitrage factor-augmented VAR approach," *Journal of Econometrics*, 146, 26–43.

Niu, L. and Zeng, G. (2012), "The Discrete-Time Framework of Arbitrage-Free Nelson-Siegel Class of Term Structure Models," *manuscript*, 1–68.

Smith, J. and Wallis, K. F. (2009), "A simple explanation of the forecast combination puzzle*," *Oxford Bulletin of Economics and Statistics*, 71, 331–355.

Stock, J. H. and Watson, M. W. (2004), "Combination forecasts of output growth in a seven-country data set," *Journal of Forecasting*, 23, 405–430.

Waggoner, D. and Zha, T. (2012), "Confronting model misspecification in macroeconomics," *Journal of Econometrics*, 171(2), 167–184.

Winkler, R. L. and Clemen, R. T. (1992), "Sensitivity of weights in combining forecasts," *Operations Research*, 40, 609–614.

Zantedeschi, D., Damien, P., and Polson, N. G. (2011), "Predictive Macro-Finance With Dynamic Partition Models," *Journal of the American Statistical Association*, 106(494), 427–439.

Appendix

A Likelihood

This section presents the step by step procedure for the log likelihood calculation. Suppose that $\boldsymbol{\psi}$ is the set of all model parameters and the log likelihood $\mathsf{log}\, L$ is initialized at 0. At time 1, $p(s_{t-1}|Y_{t-1}, \boldsymbol{\psi})$ is given at the unconditional probability of regime s_t. For $t = 1, 2, .., T$, the following steps are sequentially repeated.

Algorithm 2: Log likelihood calculation

- Step 1: The predictive probability of regime s_t, $p(s_t = j|Y_{t-1}, \boldsymbol{\psi})$ is computed as

$$\begin{aligned} p(s_t &= j|Y_{t-1}, \boldsymbol{\psi}) \\ &= \sum_{i=1}^{2} \mathsf{Pr}[s_t = j|s_{t-1} = i, \boldsymbol{\psi}] \times \mathsf{Pr}(s_{t-1} = i|Y_{t-1}, \boldsymbol{\psi}) \\ &= \sum_{i=1}^{2} q_{ij} \times p(s_{t-1} = i|Y_{t-1}, \boldsymbol{\psi}), \;\; j = 1, 2 \end{aligned}$$

- Step 2: The predictive model weight on $\mathcal{M}_1$, w_{1,s_t} is given by

$$W_{1,t} = \sum_{s_t=1}^{2} w_{1,s_t} \times p(s_t|Y^o_{t-1}, \boldsymbol{\psi})$$

  so the predictive model weight on $\mathcal{M}_2$ is $W_{2,t} = 1 - W_{1,t}$.

- Step 3: We now have the conditional likelihood density $p(\mathbf{y}_t|Y_{t-1}, \boldsymbol{\psi})$ as

$$W_{1,t} \times p(\mathbf{y}_t|Y_{t-1}, \Theta_1, \mathcal{M}_1) + W_{2,t} \times p(\mathbf{y}_t|Y_{t-1}, \Theta_2, \mathcal{M}_2),$$

  and $\mathsf{log}\, L = \mathsf{log}\, L + \mathsf{log}\, p(\mathbf{y}_t|Y_{t-1}, \boldsymbol{\psi})$

- Step 4: The updated probability of regime s_t, $p(s_t = i|Y_t, \boldsymbol{\psi})$ is calculated and retained as

$$\begin{aligned} p(s_t &= i|Y_t, \boldsymbol{\psi}) \\ &= p(s_t = i|Y_{t-1}, \boldsymbol{\psi}, \mathbf{y}_t) \\ &= \frac{p(s_t = i, \mathbf{y}_t|Y_{t-1}, \boldsymbol{\psi})}{p(\mathbf{y}_t|Y_{t-1}, \boldsymbol{\psi})} \end{aligned}$$

$$= \frac{p(\mathbf{y}_t|Y_{t-1},\boldsymbol{\psi},s_t=i)p(s_t=i|Y_{t-1},\boldsymbol{\psi})}{p(\mathbf{y}_t|Y_{t-1},\boldsymbol{\psi})} \text{ for } i=1,2$$

where the predictive density of y_t given s_t is simply given by

$$\begin{aligned} & p(y_t|Y_{t-1},\boldsymbol{\psi},s_t) \\ = \; & w_{1,s_t} \times p(\mathbf{y}_t|Y_{t-1},\Theta_1,\mathcal{M}_1) + (1-w_{1,s_t}) \times p(\mathbf{y}_t|Y_{t-1},\Theta_2,\mathcal{M}_2) \end{aligned}$$

- Step 5: $t = t+1$ and go to Step 1 if $t \leq T$

B Details of MCMC Sampling

We now discuss the details of each MCMC step. The burn-in is 1,000 and the MCMC simulation size beyond the burn-in is 10,000.

B.1 Parameters Sampling

First, $\Theta = (\Theta_{NS}, \Theta_{AF}, \Theta_{RW}, w)$ are simulated by the tailored randomized blocking Metropolis-Hastings algorithm (TaRB-MH, Chib and Ramamurthy (2010)). We note that the posterior density of Θ is proportional to the product of the likelihood and the prior because

$$\pi\left(\Theta|\mathbf{Y},Q\right) \propto f\left(\mathbf{Y}|\boldsymbol{\psi}\right) \times \pi(\Theta). \tag{B.1}$$

We simulate $\Theta|\mathbf{Y},Q$ rather than $\Theta|\mathbf{Y},\mathbf{S},\mathbf{X},Q$ by integrating out the regimes and latent factors because the former is more efficient than the latter. The likelihood computation is illustrated in Appendix A.

In every MCMC iteration, we apply the TaRB-MH method and sample Θ given $(\mathbf{Y},Q)$. This algorithm is particularly useful when the posterior density is high-dimensional and its surface is possibly irregular. For the technical details, refer to Chib and Ramamurthy (2010) or Chib and Kang (2013).

Next, because the transition probability Q is independent of $(\mathbf{Y},\Theta)$ given the regimes $\mathbf{S}$, it is sampled from

$$Q|\mathbf{S}.$$

Moreover, its prior is conjugate, and the transition probabilities are sampled from a beta distribution.

B.2 Regime Sampling

The time-series of the regimes $\mathbf{S}$ is simulated in one block by the multi-move method (Chib (1998)). This method consists of two stages. The first stage is to calculate the

filtered probabilities, $\mathsf{Pr}(s_t|Y_t,\boldsymbol{\psi})$ as

$$\begin{aligned}\mathsf{Pr}(s_t &= j|Y_t,\boldsymbol{\psi}) = \frac{\sum_{i=1}^{2} p(\mathbf{y}_t|Y_{t-1},s_t=j,\boldsymbol{\psi})\times \mathsf{Pr}(s_t=j|s_{t-1}=i,\boldsymbol{\psi})}{\sum_{j=1}^{2}\left[\sum_{i=1}^{2} p(\mathbf{y}_t|Y_{t-1},s_t=j,\boldsymbol{\psi})\times \mathsf{Pr}(s_t=j|s_{t-1}=i,\boldsymbol{\psi})\right]} \\ &= \frac{\sum_{i=1}^{2} p(\mathbf{y}_t|Y_{t-1},s_t=j,\boldsymbol{\psi})\times q_{ij}}{\sum_{j=1}^{2}\left[\sum_{i=1}^{2} p(\mathbf{y}_t|Y_{t-1},s_t=j,\boldsymbol{\psi})\times q_{ij}\right]}\end{aligned}$$

for $j = 1, 2$. Then, the conditional density of $\mathbf{y}_t$ $p(\mathbf{y}_t|Y_{t-1}, s_t, \boldsymbol{\psi})$ is computed as the linear combination of the model-specific conditional densities of $\mathbf{y}_t$: $p(\mathbf{y}_t|Y_{t-1}, \Theta_{NS}, \mathcal{M}_{NS})$, $p(\mathbf{y}_t|Y_{t-1}, \Theta_{AF}, \mathcal{M}_{AF})$, and $p(\mathbf{y}_t|Y_{t-1}, \Theta_{RW}, \mathcal{M}_{RW})$. That is,

$$\begin{aligned}& p(\mathbf{y}_t|Y_{t-1}, s_t, \boldsymbol{\psi}) \\ =\ & w_{NS,s_t} \times p(\mathbf{y}_t|Y_{t-1}, \Theta_{NS}, \mathcal{M}_{NS}) + w_{AF,s_t} \times p(\mathbf{y}_t|Y_{t-1}, \Theta_{AF}, \mathcal{M}_{AF}) \\ & +(1 - w_{NS,s_t} - w_{AF,s_t}) \times p(\mathbf{y}_t|Y_{t-1}, \Theta_{RW}, \mathcal{M}_{RW})\end{aligned}$$

These model-specific conditional densities are already given in equations (3.5), (3.14), and (3.16).

In the second stage, $\{s_t\}_{t=1}^{T}$ is sampled through a backward recursion. The regime at time T, s_T is first drawn with the filtered probability $\mathsf{Pr}(s_T|Y_T, \boldsymbol{\psi})$. Then, conditioned on s_{t+1} we compute $\mathsf{Pr}(s_t|Y_t, s_{t+1}, \boldsymbol{\psi})$ using the filtered probabilities as the following:

$$\begin{aligned}&\mathsf{Pr}(s_t = i|Y_t, s_{t+1}, \boldsymbol{\psi}) \\ &\quad = \frac{q_{ij} \times \mathsf{Pr}[s_t = i|Y_t, \boldsymbol{\psi}]}{\sum_{i=1}^{2} q_{ij} \times \mathsf{Pr}[q_t = i|Y_t, \boldsymbol{\psi}]},\ i = 1, 2\end{aligned} \tag{B.2}$$

Now given s_{t+1}, s_t is sampled with the probability $\mathsf{Pr}(s_t|Y_t, s_{t+1}, \boldsymbol{\psi})$ for $t = T - 1, T - 2, .., 1$, which completes the regime sampling.

B.3 Factor Sampling

The latent factors $\mathbf{X}$ in the DNS model are sampled independently of $(\Theta_{AF}, \Theta_{RW}, w, Q)$. Given (Θ_{NS}, Y), $\mathbf{X}$ is typically simulated by the Carter and Kohn approach (Carter and Kohn (1994)). Meanwhile, we can exactly compute the factors $\mathbf{F} = \{\mathbf{f}_t\}_{t=1}^{T}$ in the AFNS model as

$$\mathbf{f}_t = (\mathbf{b}_B)^{-1} \times \left(\mathbf{y}_t^B - \mathbf{a}_B\right)$$

by using the basis yields and the model parameters.

B.4 Predictive Yield Curve Sampling

Each MCMC cycle is completed by sampling the posterior predictive draws given ($\mathbf{Y}$, $\mathbf{X}$, $\mathbf{F}$, $\mathbf{S}$, $\boldsymbol{\psi}$). For each posterior draw $(\mathbf{y}_T, \mathbf{x}_T, \mathbf{f}_T, s_T, \boldsymbol{\psi})$ and forecast horizon of $h = 1, 2, .., H$, we first simulate the predictive draws of the factors $\{\mathbf{x}_{T+h}, \mathbf{f}_{T+h}\}_{h=1}^{H}$. Given the factors and parameters, the model-specific predictive bond yields are generated within the individual model specifications. Next, the predictive regime $\{s_{T+h}\}_{h=1}^{H}$ is sampled by the Markov-switching process, and it determines the model weights for each forecast horizon. Finally, the predictive yield curve is computed as the linear combination of the model-specific predictive yield curves and is retained as the posterior predictive draws. The following algorithm summarizes the predictive yield curve simulation.

Algorithm 3: Posterior predictive distribution simulation

- Step 1: Sample the factors $\{\mathbf{x}_{T+h}\}_{h=1}^{H}|\mathbf{X},\Theta_{NS}$ and $\{\mathbf{f}_{T+h}\}_{h=1}^{H}|\mathbf{F},\Theta_{AF}$
- Step 2: Sample the model-specific predictive yields

$$\{\mathbf{y}_{NS,T+h}\}_{h=1}^{H}|\mathbf{X},\Theta_{NS}, \quad \{\mathbf{y}_{AF,T+h}\}_{h=1}^{H}|\mathbf{F},\Theta_{AF}, \text{ and } \{\mathbf{y}_{RW,T+h}\}_{h=1}^{H}|\mathbf{Y},\Theta_{RW}$$

- Step 3: Sample the predictive regimes, $\{s_{T+h}\}_{h=1}^{H}|\mathbf{S},Q$
- Step 4: For $h = 1, 2, .., H$, compute the predictive yield curve as

$$\begin{aligned}\mathbf{y}_{T+h} &= w_{NS,s_{T+h}} \times \mathbf{y}_{NS,T+h} + w_{AF,s_{T+h}} \times \mathbf{y}_{AF,T+h} \\ &\quad +(1 - w_{NS,s_{T+h}} - w_{AF,s_{T+h}}) \times \mathbf{y}_{RW,T+h}\end{aligned}$$

- Step 5: Retain $\{\mathbf{y}_{T+h}\}_{h=1}^{H}$ as a posterior predictive draw

B.5 Figure and Tables

Table 1: List of model combinations

	DNS	AFNS	RW
Single			
DNS	◯	×	×
AFNS	×	◯	×
RW	×	×	◯
Constant weight			
NS-AF-*Const*	◯	◯	×
NS-RW-*Const*	◯	×	◯
AF-RW-*Const*	×	◯	◯
NS-AF–RW-*Const*	◯	◯	◯
NS-AF -*Equal*	◯	◯	×
NS-RW-*Equal*	◯	×	◯
AF-RW-*Equal*	×	◯	◯
NS-AF-RW-*Equal*	◯	◯	◯
Markov-switching weight			
NS-AF-*MS*	◯	◯	×
NS-RW-*MS*	◯	×	◯
AF-RW-*MS*	×	◯	◯
NS-AF-RW-*MS*	◯	◯	◯

Note: ◯ indicates the inclusion of the individual model in the pool.

Table 2: Prior

Parameter	Density	Mean	S.D.
$1200 \times \kappa$	Normal	(0.2, -0.1, -0.1)'	(0.01, 0.01, 0.01)'
diag(ϕ)	Normal	(0.9, 0.9, 0.9)'	(0.05, 0.05, 0.05)'
$1200 \times$diag(V_{NS})	Inverse Gamma	1.000	0.200
$\rho_{NS,ij}$ $(i \neq j,\ i,j = 1,2,3)$	Uniform	0.000	0.580
$1.4 \times 10^4 \times diag(\Sigma_{NS})$	Inverse Gamma	2.000	0.300

(a) DNS

Parameter	Density	Mean	S.D.
$\bar{\gamma}$	Normal	(-0.15, -0.07, 0)'	(0.01, 0.01, 0.01)'
$\boldsymbol{g}^Q$	Normal	0.067	0.031
diag(G)	Normal	(0.9, 0.9, 0.9)'	(0.05, 0.05, 0.05)'
$10^4 \times$diag(V_{AF})	Inverse Gamma	(2, 2.5, 5)'	(0.25, 0.25, 0.25)'
$\rho_{AF,ij}$ $(i \neq j,\ i,j = 1,2,3)$	Uniform	0.000	0.580
$1.4 \times 10^4 \times diag(\Sigma_{AF})$	Inverse gamma	2.000	0.300

(b) AFNS

$1.4 \times 10^4 \times diag(\Sigma_{RW})$	Inverse gamma	2.000	0.300

(c) Random-walk

w_{i,s_t} $(s_t = 1,2)$	Uniform	0.500	0.29

(d) Model weights

q_{ii} $(i = 1,2)$	Beta	0.900	0.05

(e) Transition probability

Note: $\rho_{NS,ij}$ *and* $\rho_{AF,ij}$ are the (i,j) elements of Γ_{NS} and Γ_{AF}, respectively.

Figure 1: Posterior probabilities of regime 2

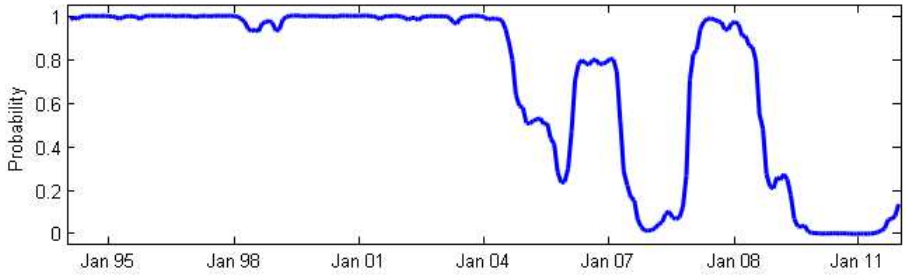

(a) NS-AF-RW-*MS*

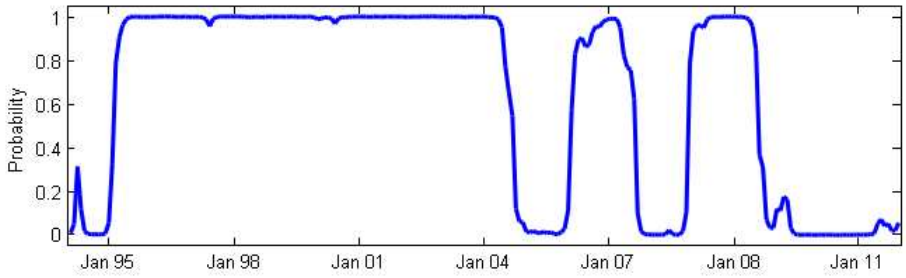

(b) NS-AF-*MS*

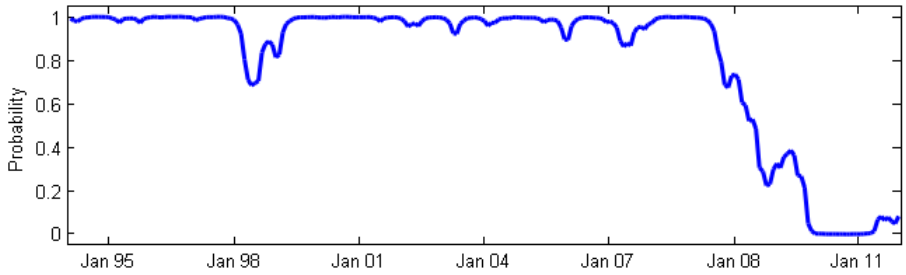

(c) NS-RW-*MS*

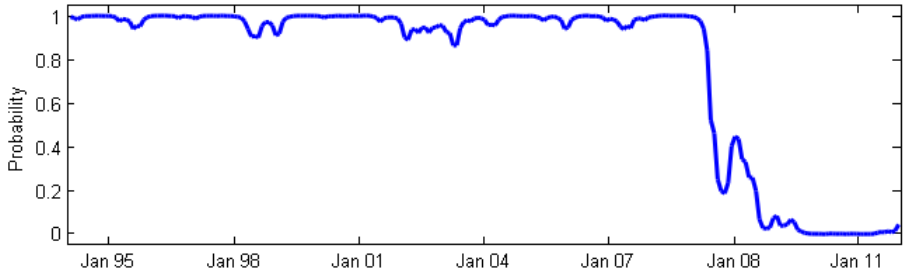

(d) AF-RW-*MS*

Note: The solid line is the posterior probability of regime 2.

Table 3: Rolling Windows: in-sample and out-of-sample

	In-sample	Out-of-sample
1	Feb. 1994 - Jan. 2004	Feb. 2004 - Jan. 2005
2	Mar. 1994 - Feb. 2004	Mar. 2004 - Feb. 2005
3	April 1994 - Mar. 2004	April 2004 - Mar. 2005
	⋮	⋮
54	Aug. 1997 - July 2008	Aug. 2008 - July 2009
55	Sept. 1997 - Aug. 2008	Sept. 2008 - Aug. 2009
	⋮	⋮
107	Dec. 2002 - Nov. 2012	Dec. 2012 - Nov. 2013
108	Jan. 2003 - Dec. 2012	Jan. 2013 - Dec. 2013

Table 4: Best models: PPC

	3m	6m	12m	24m	36m	60m	84m	120m
1-month-ahead	NR_E	NR_E	NR_E	NR_E	NR_E	AR_E	AR_E	AR_E
2-month-ahead	NR_E	NR_E	NR_E	NR_E	NR_E	AR_E	NR_E	AR_E
3-month-ahead	NR_E	NR_E	NR_E	NR_E	NR_E	AR_E	NR_E	NR_E
4-month-ahead	NR_E	NR_E	NR_E	NR_E	NR_E	NAR_E	NR_E	NR_E
5-month-ahead	NR_E	NR_E	NR_E	NR_E	NR_E	NAR_E	NR_E	NAR_E
6-month-ahead	NR_E	NR_E	NR_E	NR_E	NR_E	NAR_E	NR_E	NAR_E
7-month-ahead	NR_E	NR_E	NR_E	NR_E	NR_E	NAR_E	NR_E	NAR_E
8-month-ahead	NR_E	NR_E	NR_E	NR_E	NR_E	NAR_E	NR_E	NAR_E
9-month-ahead	NR_E	NR_E	NR_E	NR_E	NR_E	NAR_E	NR_E	NAR_E
10-month-ahead	NR_E	NR_E	NR_E	NR_E	NR_E	NAR_E	NR_E	NAR_E
11-month-ahead	NR_E	NR_E	NR_E	NR_E	NR_E	NAR_E	NR_E	NAR_E
12-month-ahead	NR_E	NR_E	NR_E	NR_E	NR_E	NAR_E	NR_E	NAR_E

Note: NR_E, AR_E, and NAR_E indicate NS-RW-*Equal*, AF-RW-*Equal*, and NS-AF-RW-*Equal*, respectively.

Table 5: One- and three-month ahead density forecast evaluations: PPC

	3m	6m	12m	24m	36m	60m	84m	120m
DNS	1.112	1.209	1.124	1.102	1.320	1.408	1.267	1.032
AFNS	4.596	4.583	3.627	2.200	1.777	1.469	1.216	0.795
RW	1.000	1.000	1.000	1.000	1.000	1.000	1.000	1.000
NS-AF -*Equal*	1.790	1.671	1.300	1.043	1.158	1.035	1.140	0.767
NS-AF-*Const*	1.116	1.102	0.956	0.937	1.081	1.027	1.051	0.846
NS-AF-*MS*	1.941	1.980	1.655	1.310	1.272	1.116	1.146	0.931
NS-RW-*Equal*	**0.749**	**0.708**	**0.653**	**0.677**	**0.748**	**0.779**	**0.752**	**0.676**
NS-RW-*Const*	0.957	0.983	0.931	0.952	1.088	1.128	1.042	0.882
NS-RW-*MS*	0.887	0.907	0.850	0.870	0.978	0.999	0.945	0.833
AF-RW-*Equal*	1.655	1.615	1.319	0.953	0.853	0.736	0.750	0.620
AF-RW-*Const*	3.095	3.047	2.438	1.586	1.345	1.118	1.048	0.749
AF-RW-*MS*	2.719	2.578	1.990	1.310	1.089	0.934	0.901	0.670
NS-AF-RW-*Equal*	1.413	1.329	1.116	0.982	1.018	0.904	1.009	0.791
NS-AF-RW-*Const*	1.141	1.109	1.023	1.049	1.197	1.168	1.193	0.940
NS-AF-RW-*MS*	1.676	1.730	1.570	1.372	1.402	1.296	1.401	1.163

(a) One-month-ahead

	3m	6m	12m	24m	36m	60m	84m	120m
DNS	1.113	1.047	1.024	1.074	1.152	1.175	1.106	1.000
AFNS	3.964	3.657	3.004	2.043	1.657	1.170	1.138	0.839
RW	1.000	1.000	1.000	1.000	1.000	1.000	1.000	1.000
NS-AF -*Equal*	1.680	1.501	1.259	1.077	1.082	0.966	1.023	0.818
NS-AF-*Const*	1.099	1.005	0.937	0.949	0.990	0.915	0.929	0.824
NS-AF-*MS*	1.685	1.558	1.354	1.166	1.098	0.924	0.947	0.837
NS-RW-*Equal*	**0.806**	**0.769**	**0.743**	**0.733**	**0.747**	**0.741**	**0.717**	**0.661**
NS-RW-*Const*	0.988	0.950	0.937	0.974	1.022	1.029	0.978	0.887
NS-RW-*MS*	0.910	0.882	0.864	0.887	0.924	0.927	0.891	0.826
AF-RW-*Equal*	1.558	1.474	1.282	1.002	0.897	0.724	0.767	0.663
AF-RW-*Const*	2.753	2.567	2.163	1.577	1.346	1.006	1.052	0.832
AF-RW-*MS*	2.453	2.229	1.807	1.320	1.114	0.859	0.922	0.760
NS-AF-RW-*Equal*	1.211	1.126	1.007	0.882	0.853	0.733	0.802	0.688
NS-AF-RW-*Const*	0.992	0.929	0.894	0.909	0.943	0.894	0.901	0.790
NS-AF-RW-*MS*	1.210	1.158	1.074	1.000	0.991	0.894	0.939	0.833

(b) Three-month-ahead

Note: Bold entries indicate the best density forecasting performance for each maturity and forecast horizon.

Table 6: Six- and twelve-month ahead density forecast evaluations: PPC

	3m	6m	12m	24m	36m	60m	84m	120m
DNS	1.103	1.045	1.027	1.047	1.096	1.077	1.023	0.937
AFNS	3.261	3.072	2.666	1.969	1.646	1.107	1.123	0.855
RW	1.000	1.000	1.000	1.000	1.000	1.000	1.000	1.000
NS-AF -*Equal*	1.473	1.378	1.233	1.079	1.061	0.920	0.969	0.805
NS-AF-*Const*	1.085	1.028	0.981	0.957	0.968	0.871	0.883	0.799
NS-AF-*MS*	1.469	1.399	1.283	1.134	1.064	0.874	0.895	0.798
NS-RW-*Equal*	**0.847**	**0.834**	**0.805**	**0.747**	**0.739**	0.712	**0.693**	0.644
NS-RW-*Const*	0.998	0.975	0.968	0.966	0.988	0.963	0.922	0.839
NS-RW-*MS*	0.932	0.909	0.893	0.881	0.900	0.882	0.856	0.795
AF-RW-*Equal*	1.397	1.359	1.237	0.998	0.894	0.703	0.746	0.649
AF-RW-*Const*	2.337	2.230	1.984	1.543	1.340	0.956	1.023	0.826
AF-RW-*MS*	2.082	1.945	1.672	1.296	1.117	0.825	0.904	0.758
NS-AF-RW-*Equal*	1.068	1.039	0.969	0.848	0.800	**0.660**	0.706	**0.619**
NS-AF-RW-*Const*	0.939	0.914	0.900	0.884	0.890	0.809	0.811	0.729
NS-AF-RW-*MS*	1.050	1.028	0.987	0.926	0.907	0.799	0.822	0.738

(a) Six-month-ahead

	3m	6m	12m	24m	36m	60m	84m	120m
DNS	1.089	1.045	1.037	1.064	1.100	1.065	0.995	0.929
AFNS	2.468	2.394	2.229	1.873	1.660	1.161	1.152	0.894
RW	1.000	1.000	1.000	1.000	1.000	1.000	1.000	1.000
NS-AF -*Equal*	1.203	1.169	1.120	1.058	1.045	0.907	0.915	0.788
NS-AF-*Const*	1.046	1.011	0.994	0.988	0.991	0.890	0.867	0.804
NS-AF-*MS*	1.225	1.196	1.161	1.107	1.070	0.902	0.894	0.822
NS-RW-*Equal*	**0.884**	**0.870**	**0.844**	**0.769**	**0.733**	0.663	**0.618**	0.572
NS-RW-*Const*	0.989	0.970	0.968	0.965	0.973	0.925	0.861	0.792
NS-RW-*MS*	0.940	0.918	0.913	0.900	0.903	0.859	0.808	0.751
AF-RW-*Equal*	1.195	1.181	1.125	0.966	0.869	0.659	0.664	0.568
AF-RW-*Const*	1.786	1.748	1.654	1.428	1.288	0.933	0.948	0.764
AF-RW-*MS*	1.635	1.574	1.448	1.231	1.090	0.788	0.828	0.690
NS-AF-RW-*Equal*	0.941	0.942	0.926	0.854	0.797	**0.635**	0.636	**0.556**
NS-AF-RW-*Const*	0.932	0.917	0.921	0.914	0.909	0.813	0.782	0.710
NS-AF-RW-*MS*	0.966	0.958	0.958	0.931	0.907	0.788	0.773	0.701

(b) 12-month-ahead

Note: Bold entries indicate the best density forecasting performance for each maturity and forecast horizon.

Table 7: Best Models: RMSE

	3m	6m	12m	24m	36m	60m	84m	120m
1-month-ahead	R	NR_E	NR_M	R	R	R	R	NR_M
2-month-ahead	R	N	N	R	R	R	R	NA_M
3-month-ahead	R	N	N	R	R	R	R	NA_C
4-month-ahead	R	N	N	R	R	R	R	NA_C
5-month-ahead	R	N	N	R	R	R	R	NA_C
6-month-ahead	R	N	N	R	R	R	R	NA_M
7-month-ahead	R	R	N	R	R	R	R	R
8-month-ahead	R	R	R	R	R	R	R	R
9-month-ahead	R	NR_M	R	R	R	R	R	R
10-month-ahead	R	NR_M	R	R	R	R	R	R
11-month-ahead	R	NR_M	R	R	R	R	R	R
12-month-ahead	R	NR_M	R	R	R	R	R	R

Note: N, R, NR_E, NR_M, NA_C, and NA_M indicate DNS, RW, NS-RW-*Equal*, NS-RW-*MS*, NS-AF-*Const*, and NS-AF-*MS*, respectively.

Table 8: One- and three-month-ahead point forecast evaluations: RMSE

	3m	6m	12m	24m	36m	60m	84m	120m
DNS	1.036	1.007	0.905	1.043	1.232	1.326	1.206	1.006
AFNS	1.074	1.079	0.983	1.112	1.227	1.101	1.272	1.047
RW	**1.000**	1.000	1.000	**1.000**	**1.000**	**1.000**	**1.000**	1.000
NS-AF -*Equal*	1.178	1.124	1.010	1.155	1.342	1.294	1.385	1.079
NS-AF-*Const*	1.090	1.040	0.925	1.058	1.207	1.163	1.196	1.005
NS-AF-*MS*	1.257	1.273	1.173	1.230	1.279	1.145	1.253	1.079
NS-RW-*Equal*	1.027	**0.980**	0.927	1.035	1.098	1.133	1.086	**0.998**
NS-RW-*Const*	1.039	1.001	0.913	1.052	1.177	1.234	1.147	1.001
NS-RW-*MS*	1.021	0.990	**0.904**	1.028	1.126	1.162	1.101	0.998
AF-RW-*Equal*	1.083	1.081	1.029	1.098	1.125	1.036	1.145	1.040
AF-RW-*Const*	1.154	1.158	1.079	1.174	1.244	1.112	1.279	1.093
AF-RW-*MS*	1.138	1.106	1.008	1.142	1.173	1.075	1.222	1.063
NS-AF-RW-*Equal*	1.274	1.236	1.166	1.271	1.338	1.252	1.354	1.163
NS-AF-RW-*Const*	1.275	1.239	1.164	1.276	1.388	1.368	1.374	1.157
NS-AF-RW-*MS*	1.450	1.468	1.400	1.435	1.481	1.416	1.474	1.278

(a) One-month-ahead

	3m	6m	12m	24m	36m	60m	84m	120m
DNS	1.045	**0.974**	**0.942**	1.057	1.131	1.186	1.128	1.017
AFNS	1.150	1.125	1.092	1.180	1.223	1.059	1.251	1.108
RW	**1.000**	1.000	1.000	**1.000**	**1.000**	**1.000**	**1.000**	1.000
NS-AF -*Equal*	1.218	1.144	1.085	1.176	1.252	1.235	1.299	1.136
NS-AF-*Const*	1.103	1.023	0.976	1.064	1.114	1.079	1.100	**0.993**
NS-AF-*MS*	1.203	1.136	1.073	1.132	1.143	1.048	1.104	1.008
NS-RW-*Equal*	1.036	0.998	0.986	1.050	1.070	1.092	1.063	0.998
NS-RW-*Const*	1.054	1.007	0.987	1.085	1.134	1.174	1.129	1.035
NS-RW-*MS*	1.022	0.985	0.962	1.045	1.084	1.115	1.081	1.012
AF-RW-*Equal*	1.106	1.093	1.079	1.130	1.140	1.067	1.160	1.087
AF-RW-*Const*	1.215	1.194	1.174	1.245	1.268	1.141	1.301	1.181
AF-RW-*MS*	1.168	1.128	1.085	1.170	1.180	1.090	1.235	1.141
NS-AF-RW-*Equal*	1.155	1.109	1.082	1.142	1.161	1.108	1.185	1.088
NS-AF-RW-*Const*	1.139	1.077	1.046	1.123	1.159	1.146	1.153	1.043
NS-AF-RW-*MS*	1.183	1.135	1.100	1.159	1.179	1.142	1.179	1.078

(b) Three-month-ahead

Note: Bold entries indicate the best point forecasting performance for each maturity and forecast horizon.

Table 9: Six- and twelve-month ahead point forecast evaluations: RMSE

	3m	6m	12m	24m	36m	60m	84m	120m
DNS	1.039	**0.997**	**0.986**	1.062	1.127	1.153	1.104	1.009
AFNS	1.125	1.127	1.131	1.211	1.265	1.084	1.277	1.159
RW	**1.000**	1.000	1.000	**1.000**	**1.000**	**1.000**	**1.000**	1.000
NS-AF -*Equal*	1.169	1.139	1.123	1.193	1.261	1.225	1.286	1.158
NS-AF-*Const*	1.091	1.052	1.031	1.085	1.123	1.074	1.091	1.001
NS-AF-*MS*	1.154	1.120	1.095	1.133	1.144	1.037	1.078	**0.988**
NS-RW-*Equal*	1.029	1.017	1.016	1.055	1.081	1.088	1.069	1.014
NS-RW-*Const*	1.044	1.023	1.025	1.097	1.144	1.164	1.127	1.044
NS-RW-*MS*	1.018	0.998	0.995	1.054	1.095	1.114	1.089	1.025
AF-RW-*Equal*	1.076	1.081	1.088	1.133	1.156	1.074	1.162	1.098
AF-RW-*Const*	1.160	1.163	1.177	1.255	1.297	1.154	1.310	1.210
AF-RW-*MS*	1.128	1.115	1.105	1.178	1.206	1.099	1.244	1.164
NS-AF-RW-*Equal*	1.079	1.068	1.066	1.110	1.130	1.056	1.119	1.044
NS-AF-RW-*Const*	1.075	1.050	1.045	1.099	1.131	1.092	1.097	1.013
NS-AF-RW-*MS*	1.080	1.062	1.060	1.113	1.140	1.088	1.113	1.032

(a) Six-month-ahead

	3m	6m	12m	24m	36m	60m	84m	120m
DNS	1.031	1.008	1.017	1.107	1.190	1.249	1.200	1.127
AFNS	1.070	1.084	1.119	1.244	1.347	1.242	1.426	1.334
RW	**1.000**	1.000	**1.000**	**1.000**	**1.000**	**1.000**	**1.000**	**1.000**
NS-AF -*Equal*	1.081	1.074	1.090	1.189	1.285	1.305	1.358	1.272
NS-AF-*Const*	1.065	1.044	1.049	1.120	1.181	1.169	1.167	1.102
NS-AF-*MS*	1.084	1.071	1.079	1.148	1.198	1.144	1.166	1.100
NS-RW-*Equal*	1.019	1.011	1.022	1.068	1.109	1.129	1.099	1.054
NS-RW-*Const*	1.024	1.013	1.030	1.112	1.183	1.232	1.188	1.122
NS-RW-*MS*	1.004	**0.992**	1.006	1.078	1.142	1.185	1.149	1.091
AF-RW-*Equal*	1.026	1.032	1.054	1.120	1.170	1.117	1.190	1.134
AF-RW-*Const*	1.066	1.078	1.116	1.230	1.318	1.241	1.378	1.298
AF-RW-*MS*	1.059	1.059	1.073	1.162	1.221	1.145	1.287	1.226
NS-AF-RW-*Equal*	1.018	1.022	1.045	1.114	1.158	1.108	1.146	1.082
NS-AF-RW-*Const*	1.042	1.031	1.048	1.123	1.180	1.175	1.161	1.090
NS-AF-RW-*MS*	1.030	1.024	1.047	1.123	1.175	1.155	1.162	1.095

(b) 12-month-ahead

Note: Bold entries indicate the best point forecasting performance for each maturity and forecast horizon.

Table 10: Best models: pre-crisis period

	3m	6m	12m	24m	36m	60m	84m	120m
1-month-ahead	NR_E	NR_E	NR_E	NR_E	NR_E	NAR_E	AR_E	AR_E
2-month-ahead	NAR_C	NAR_C	NR_E	NAR_E	NAR_E	NAR_E	AR_E	AR_E
3-month-ahead	NAR_C	NAR_C	NAR_E	NAR_E	NAR_E	NAR_E	AR_E	AR_E
4-month-ahead	NAR_C	NAR_C	NAR_E	NAR_E	NAR_E	NAR_E	AR_E	AR_E
5-month-ahead	NAR_C	NAR_C	NAR_E	NAR_E	NAR_E	NAR_E	AR_E	AR_E
6-month-ahead	NAR_C	NAR_C	NAR_E	NAR_E	NAR_E	NAR_E	AR_E	AR_E
7-month-ahead	NAR_C	NAR_C	NAR_E	NAR_E	NAR_E	NAR_E	AR_E	AR_E
8-month-ahead	NAR_C	NAR_C	NAR_E	NAR_E	NAR_E	NAR_E	AR_E	AR_E
9-month-ahead	NAR_C	NAR_C	NAR_E	NAR_E	NAR_E	NAR_E	AR_E	AR_E
10-month-ahead	NAR_M	NAR_M	NAR_E	NAR_E	NAR_E	NAR_E	AR_E	AR_E
11-month-ahead	NAR_M	NAR_M	NAR_E	NAR_E	NAR_E	NAR_E	AR_E	AR_E
12-month-ahead	NAR_E	NAR_E	NAR_E	NAR_E	NAR_E	AR_E	AR_E	AR_E

(a) PPC

	3m	6m	12m	24m	36m	60m	84m	120m
1-month-ahead	NAR_M	NAR_E	NAR_E	NA_C	NAR_M	NAR_M	R	NA_C
2-month-ahead	NAR_E	NAR_E	NA_E	NAR_E	NAR_M	NAR_M	NAR_M	NA_C
3-month-ahead	NAR_E	NAR_E	NA_E	NAR_E	NAR_M	NAR_M	NAR_C	NAR_C
4-month-ahead	NAR_E	NAR_E	NAR_E	NAR_E	NAR_M	NAR_M	NAR_C	NA_C
5-month-ahead	NAR_E	NAR_E	NAR_E	NAR_E	NAR_E	A	NAR_C	NAR_C
6-month-ahead	NAR_E	NAR_E	NAR_E	NAR_E	NAR_M	A	R	NAR_C
7-month-ahead	NAR_E	NAR_E	NAR_E	NAR_E	NAR_E	A	R	NR_M
8-month-ahead	NAR_E	NA_E	A	A	NAR_M	A	R	R
9-month-ahead	A	A	A	A	NAR_E	A	R	R
10-month-ahead	A	NA_E	A	A	NAR_E	A	R	R
11-month-ahead	A	A	A	A	NAR_E	A	R	R
12-month-ahead	A	A	A	A	A	A	R	R

(b) RMSE

Note: A, N, R, NR_E, NR_M, NA_C, NA_M, AR_E, NAR_E, NAR_C, and NAR_M indicate AFNS, DNS, RW, NS-RW-*Equal*, NS-RW-*MS*, NS-AF-*Const*, NS-AF-*MS*, AF-RW-*Equal*, NS-AF-RW-*Equal*, NS-AF-RW-*Const*, and NS-AF-RW-*MS*, respectively. These models are chosen based on the first 54 out-of-sample predictions ranging from February 1994 to July 2009.

Table 11: Best models: post-crisis period

	3m	6m	12m	24m	36m	60m	84m	120m
1-month-ahead	NR_E	NR_E	NR_E	NR_E	NR_E	AR_E	NR_E	AR_E
2-month-ahead	NR_E	NR_E	NR_E	NR_E	NR_E	AR_E	NR_E	NR_E
3-month-ahead	NR_E	NR_E	NR_E	NR_E	NR_E	AR_E	NR_E	NR_E
4-month-ahead	NR_E	NR_E	NR_E	NR_E	NR_E	NR_E	NR_E	NR_E
5-month-ahead	NR_E	NR_E	NR_E	NR_E	NR_E	NAR_E	NR_E	NR_E
6-month-ahead	NR_E	NR_E	NR_E	NR_E	NR_E	NAR_E	NR_E	NAR_E
7-month-ahead	NR_E	NR_E	NR_E	NR_E	NR_E	NAR_E	NR_E	NAR_E
8-month-ahead	NR_E	NR_E	NR_E	NR_E	NR_E	NAR_E	NR_E	NAR_E
9-month-ahead	NR_E	NR_E	NR_E	NR_E	NR_E	NAR_E	NR_E	NAR_E
10-month-ahead	NR_E	NR_E	NR_E	NR_E	NR_E	NAR_E	NR_E	NAR_E
11-month-ahead	NR_E	NR_E	NR_E	NR_E	NR_E	NR_E	NR_E	NAR_E
12-month-ahead	NR_E	NR_E	NR_E	NR_E	NR_E	NR_E	NR_E	NAR_E

(a) PPC

	3m	6m	12m	24m	36m	60m	84m	120m
1-month-ahead	R	N	NR_M	R	R	R	R	NR_E
2-month-ahead	R	N	N	R	R	R	R	NA_M
3-month-ahead	R	N	N	R	R	R	R	NR_E
4-month-ahead	R	R	R	R	R	R	R	R
5-month-ahead	R	R	R	R	R	R	R	NA_M
6-month-ahead	R	R	R	R	R	R	R	NA_M
7-month-ahead	R	R	R	R	R	R	R	NA_M
8-month-ahead	R	R	R	R	R	R	R	R
9-month-ahead	R	R	R	R	R	R	R	R
10-month-ahead	R	R	R	R	R	R	R	R
11-month-ahead	R	R	R	R	R	R	R	R
12-month-ahead	R	R	R	R	R	R	R	R

(b) RMSE

Note: N, R, NR_E, NR_M, NA_M, AR_E, and NAR_E indicate DNS, RW, NS-RW-*Equal*, NS-RW-*MS*, NS-AF-*MS*, AF-RW-*Equal*, and NS-AF-RW-*Equal*, respectively. These models are chosen based on the recent 54 out-of-sample predictions ranging from September 2008 to December 2013.

Table 12: Constant model weight estimates

	DNS	AFNS	RW
NS-AF-*Const*	0.678	0.322	-
	(0.034)	(0.034)	
NS-RW-*Const*	0.749	-	0.251
	(0.029)		(0.029)
AF-RW-*Const*	-	0.702	0.298
		(0.033)	(0.033)
NS-AF-RW-*Const*	0.593	0.181	0.226
	(0.034)	(0.027)	(0.028)

Note: Standard errors are in parentheses.

Table 13: Markov-switching model weight estimates

	Regime 1 ($s_t = 1$)			Regime 2 ($s_t = 2$)		
	DNS	AFNS	RW	DNS	AFNS	RW
NS-AF-*MS*	0.216	0.784	-	0.883	0.117	-
	(0.048)	(0.048)		(0.015)	(0.015)	
NS-RW-*MS*	0.339	-	0.661	0.858	-	0.142
	(0.080)		(0.080)	(0.027)		(0.027)
AF-RW-*MS*	-	0.276	0.724	-	0.834	0.166
		(0.068)	(0.068)		(0.030)	(0.030)
NS-AF-RW-*MS*	0.219	0.352	0.429	0.752	0.115	0.133
	(0.051)	(0.060)	(0.062)	(0.027)	(0.014)	(0.023)

Note: Standard errors are in parentheses.